Wetting properties of simple binary mixtures and systems with one self-associating component

C. Pérez, P. Roquero, and V. Talanquer[a)]
Facultad de Química, Universidad Nacional Autónoma de México, Cd. Universitaria, México D. F. 04510, México

(Received 8 July 1993; accepted 6 January 1994)

The presence of additional chemical equilibria in an otherwise simple system can induce unexpected phase behavior. We analyze the effect of this phenomenon on the wetting properties of binary mixtures with one self-associating component. As a first step we characterize the global wetting phase diagram of a mean-field lattice model for a simple binary system. We evaluate its reliability in generating an adequate topological description of bulk critical and wetting transition manifolds. These results serve as a basis to study the influence of self-association. We find that under appropriate conditions the appearance of new species in solution can lead to irregular wetting behavior such as "reentrant" wetting and "dewetting."

I. INTRODUCTION

Since 1977, when the concept of wetting transitions was introduced independently by Cahn[1] and Ebner and Sam,[2] a considerable amount of theoretical and experimental effort has been devoted to extend, restrict, or test their initial predictions. The work based on lattice-type and continuous models has shown the delicate dependence of interfacial properties on microscopic details. The experimental observation of wetting transitions, although successful, has proved to be more difficult than was expected. The link between the results in both areas is not always easy as there are problems associated with gravity effects, finite size samples, purity of components, equilibrium conditions, relaxation times, and cell geometry. Hence, wetting has become a whole area of continuous research.[3,4]

Among the different kinds of theoretical approaches to the wetting phenomena, global analyses of possible wetting behaviors have been particularly fruitful.[5–9] When considering wetting at fluid interfaces, these studies suggest that the particular characteristics of the coexisting phases tend to determine the interfacial behavior, and the structure of the phase diagram is especially relevant. Recently, it has been shown that the presence of a "chemical" equilibrium among the species in the medium can lead to "unexpected" phase transitions and critical phenomena.[10,11] One can surmise then that this kind of process might intervene to alter the wetting evolution. Working under this assumption, we will consider the problem of binary mixtures with one self-associating component. This case is important as many of the experiments on wetting at fluid interfaces have been done on systems that belong to this category.[4]

The wetting properties of our modeled self-associating system depend crucially on the corresponding properties of the related binary case where no association occurs. This is an interesting case by itself and its global wetting phase diagram will be described in detail. As a first approximation to the problem we decided to concentrate our effort in characterizing the topology and connectivity of bulk critical and wetting transition manifolds of a simple mean-field lattice model for binary mixtures. We are aware of the limitations of this approximation in describing specific details of wetting behavior such as the order of the transitions, or the evolution in prewetting regions.[4] Our results, however, lead us to conclude that the model is appropriate at the selected "structural" level of prediction. Self-associating binary systems are modeled as pseudobinary mixtures where a third species appears as a result of a chemical process regulated by a phenomenological free energy ΔG^0. Under specific circumstances the association can be responsible for "irregular" interfacial behavior: in particular, reentrant wetting and dewetting.

This paper has been arranged in the following manner. Section II is devoted to presenting the simple binary mixture model whose properties serve as a basis for dealing with the self-associating case. The first part of this section introduces the model and methodology of solution, and the second part presents and discusses the general results. In this subsection we have evaluated the adequacy of the model in representing the gross behavior of real systems. In Sec. III we address the problem of self-association in binary mixtures; the model is presented in Sec. III A and the corresponding results are to be found in Sec. III B. Here, we have sought to emphasize the most general properties. Finally we present a summary of the relevant results.

II. SIMPLE BINARY MIXTURE

A. The model

Consider a compressible binary mixture of N_x and N_y particles of species X and Y, respectively, located on the $N=N_x+N_y+N_z$ sites of a regular lattice. For uniform states the mean-field Helmholtz free energy per site f can be written as[12]

$$f=kT[x\ln x+y\ln y+z\ln z]+q(ayz+bxz+cxy)+\mu_x^0 x+\mu_y^0 y, \quad (1)$$

[a)]At The James Franck Institute, University of Chicago, Chicago, Illinois 60637 during 1994, and to whom correspondence should be addressed.

 0021-9606/94/100(8)/5913/9/$6.00

where k is the Boltzmann's constant, T is the absolute temperature, q is the coordination number, x and y are the occupation fractions of species X and Y (N_i/N; with $z=1-x-y$, the fraction of empty sites), μ_x^0 and μ_y^0 are standard chemical potentials referred to a hypothetical ideal solution state, and

$$a=\alpha_{yy}, \quad b=\alpha_{xx}, \quad \text{and} \quad c=\alpha_{xx}+\alpha_{yy}-2\alpha_{xy}$$

are a measure of first-neighbor interactions α_{ij} between ij particles in the system. This model can also be conceived as a ternary regular mixture with phenomenological energy parameters a, b, and c, or as a mean-field Blume–Emery–Griffiths (BEG) model.[13]

The free energy in Eq. (1) predicts an n-phase coexistence state for given T and chemical potentials μ_x and μ_y, provided the equation

$$\Pi(\mu_x,\mu_y)=\min(f-\mu_x x-\mu_y y) \tag{2}$$

has n minima of equal depth Π at different points on the triangle $1\geq x\geq 0$, $1\geq y\geq 0$, $1\geq x+y\geq 0$.

The condition implicit in Eq. (2) leads to the relations

$$\mu_x=kT\ \ln(x/z)+qb(z-x)+q(c-a)y+\mu_x^0, \tag{3a}$$

$$\mu_y=kT\ \ln(y/z)+qa(z-y)+q(c-b)x+\mu_y^0 \tag{3b}$$

which, together with Eq. (1), allow for the full characterization of the global phase diagram of this mean-field spin-1 Ising model. The general solutions to this problem for uniform[12] (ferromagnetic) and ordered[14] (antiferromagnetic) states are well known and we will take advantage of them to analyze the global wetting behavior.

In order to study the model surface properties, we can set the binary mixture on a cubic lattice and impose vertical boundary conditions such that equal occupancies x_i and y_i of X and Y atoms, respectively, are found within the same $x-y$ plane. Furthermore, we also demand that the uniform properties of one of two chosen coexistent phases are recovered for those planes far away from the flat interface perpendicular to the z axis. For a system with N_p planes in the vertical direction, the mean-field grand canonical potential per number of sites in a plane ω is given by

$$\omega=\sum_i^{N_p}\ (f_i-a\Delta y\Delta z-b\Delta x\Delta z-c\Delta x\Delta y-\mu_x x_i-\mu_y y_i), \tag{4}$$

where $\Delta m=m_{i+1}-m_i$ $(m=x,y,z)$, f_i is the Helmholtz free energy per plane of a homogeneous bulk phase with densities x_i and y_i, and the sum runs over all i planes.

Equation (4) has the basic structure of a discrete "square-gradient" variational functional for binary mixtures,[3,15] and its minimization as a function of the local fractions x_i and y_i leads to a set of $2N_p$ coupled equations that determine the equilibrium profile. That is,

$$\mu_x=\mu_x^i-b(\Delta^2 z-\Delta^2 x)-(c-a)\Delta^2 y, \tag{5a}$$

$$\mu_y=\mu_y^i-a(\Delta^2 z-\Delta^2 y)-(c-b)\Delta^2 x \tag{5b}$$

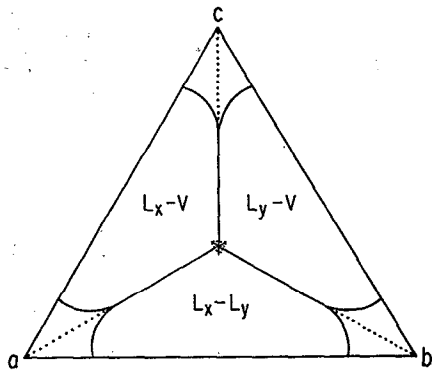

FIG. 1. Projection of the global phase diagram of the simple binary mixture onto the triangle (a, b, c). We indicate the nature of the pair of phases that become critical at critical end points.

with $\Delta^2 m=2m_i-m_{i+1}-m_{i-1}$ $(m=x,y,z)$, $\mu_x^i=\partial f_i/\partial x_i$, and $\mu_y^i=\partial f_i/\partial y_i$ define the local chemical potentials.

Equilibrium profiles between two coexisting phases can be found by proposing an initial solution for Eqs. (5) and iterating until convergence is reached; the corresponding interfacial tension γ follows directly from the excess grand potential per unit area, $\gamma=\omega-\omega_{\text{unif}}$. Wetting properties of fluid interfaces in binary mixtures that exhibit lines of triple points in the field space spanned by (T,μ_x,μ_y) can be derived by analyzing the temperature behavior of the interfacial tension for pairs of coexisting phases.[7]

B. Results

System phase diagrams for the binary mixture are completely determined by the value of the energy parameters a, b, and c. Once these are chosen, surface properties are unequivocally characterized. The global phase diagram of our binary mixture model consists of a set of phase coexistence and critical manifolds located in a five-dimensional space defined by five independent parameters[12] $(a,b,c,\mu_x,\mu_y$, for example). Since multiplying Eq. (1) by a positive factor has no influence on phase coexistence, as it only changes the working temperature scale, it is convenient to adopt the following normalization for the energy parameters[12]:

$$|a|+|b|+|c|=1. \tag{6}$$

This allows the projection of all relevant features of the global phase diagram onto the space spanned by these variables on an equilateral triangle; here a point (a,b,c), representing a particular system, is at the center of mass if masses of magnitude $|a|$, $|b|$, and $|c|$ $(=1-|a|-|b|)$ are placed at the corresponding vertices.

Systems exhibiting lines of triple points that extend from $T=0$ to a critical point of a certain nature are only to be found in the so-called principal triangle $(a>0,\ b>0,\ c>0)$. Its barycentric representation is shown in Fig. 1 where several different regions can be identified, some of them related by the symmetry properties of the basic model. Solid lines in this triangle are projections of lines of tricritical points, whereas dotted lines correspond to boundaries of manifolds of four-phase coexistence; the central region is known as the

shield zone. In those areas between solid lines, three phase coexistence states terminate at a critical end point whose temperature goes to zero as we approach the sides of the triangle.[12] No sublattice ordered phase is stable in this entire region of the energy space.[14]

In general, coexisting phases at a triple point have densities that correspond to two liquid phases with high concentration of one of two components (L_x and L_y), and one vapor-like phase (V). In Fig. 1 we have also indicated the nature of those phases that become critical at the critical end points. For $T=0$ the occupation fractions in each phase reach extreme values, and the interfacial structure between phases in coexistence is characterized by a step profile. In this limit, the only contribution to the surface tension arises from the nonlocal terms in Eq. (4) for those planes facing the discontinuity in the profile. Hence, for $T=0$, we find

$$\gamma_{L_yV}=a, \quad \gamma_{L_xV}=b, \quad \gamma_{L_xL_y}=c. \tag{7}$$

When three phase coexistence states are considered, two sets of density profiles can be obtained for each pair of possible interfaces (L_xV, L_yV, and L_xL_y). One of them is the composite of the profiles of the other two interfaces subject to the boundary conditions of the interface of interest (for L_xV, e.g., we have L_xL_y and L_yV); this solution corresponds to the presence of a wetting film. The other solution describes partial wetting. Recalling that partial wetting at a given interface, L_xV in this example, implies $\gamma_{L_xV} \leqslant \gamma_{L_xL_y} + \gamma_{L_yV}$, while perfect or complete wetting occurs whenever Antonow's law $\gamma_{L_xV} = \gamma_{L_xL_y} + \gamma_{L_yV}$ is satisfied,[16] it follows from the relations in Eq. (7) that L_y wets the L_xV interface at $T=0$ in the region of the principal triangle where $b \geqslant a+c$. When we increase the temperature, the surface tension of the interface that dissapears at the critical point approaches zero faster than the difference of surface tensions of the other two interfaces. This assures that once we have total wetting at $T=0$ ($\gamma_{L_xV} - \gamma_{L_yV} \geqslant \gamma_{L_xL_y}$ or $\gamma_{L_xV} - \gamma_{L_xL_y} \geqslant \gamma_{L_yV}$, in our example), this state remains as the preferred solution up to the critical point. Hence perfect wetting at all temperatures is to be found in those regions of the principal triangle where

$a \geqslant b+c$ (L_x wets the L_yV interface),
$b \geqslant a+c$ (L_y wets the L_xV interface),
$c \geqslant a+b$ (V "dries" the L_xL_y interface).

We will call this wetting regime of type I.

To characterize the rest of the energy space we have followed the same kind of analysis proposed by Costas *et al.*[7] in their study of the global wetting phase diagram for binary van der Waals mixtures. Different wetting regimes are identified by means of interfacial tension vs temperature plots like those sketched in Fig. 2. The principal triangle can be divided in regions that exhibit one of the four general behaviors depicted in this figure. First we identify perfect wetting at all temperatures lower than the bulk critical temperature T_c [Fig. 2(a)]; the wetting film structure always has the lowest tension (type I). In Fig. 2(b), the largest tension at low temperatures is associated to the film structure but as we approach T_c the situation is reversed and the film becomes the equilibrium state. There is a discontinuity in the slope of

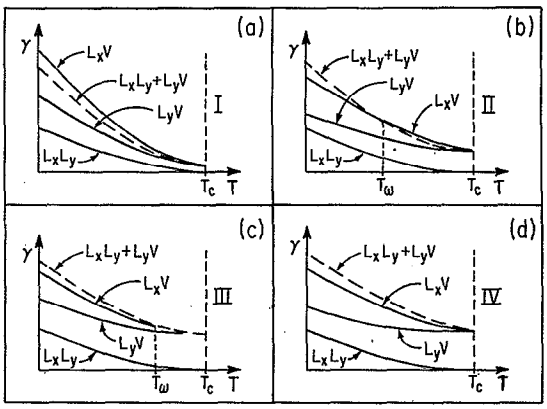

FIG. 2. Temperature behavior of interfacial tensions at three-phase coexistence states. We illustrate the four types of wetting regimes at the L_xV interface (L_y is the intruding phase). (a) Total wetting by L_y at all temperatures. (b) First-order wetting transition. (c) Second-order wetting transition. (d) Partial wetting at all temperatures.

the equilibrium tension and the surface transition at T_w is first order; both possible interfacial structures coexist at this point (type II). If the corresponding two tensions join tangentially at the transition temperature $T_w<T_c$ [Fig. 2(c)], the system is said to exhibit second-order wetting transitions; for $T \geqslant T_w$ only the film structure persists (type III). Finally, it is also possible to identify states where partial wetting remains as the only stable solution for all $T \leqslant T_c$ at any interface [type IV; Fig. 2(d)].

Figure 3 shows our results for the location of each wetting type in the barycentric representation of the principal triangle; the full characterization follows by symmetry. We have also indicated the nature of the wetting phase for systems within the region bounded by the dotted lines (type IV) and the sides of the triangle. In wetting by liquid phases, the intruding phase is always that which is rich in the less attractive particles (also the liquid with the lower number density).

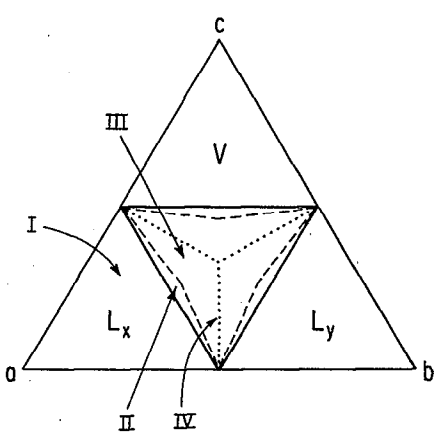

FIG. 3. Projection of the global wetting phase diagram onto the principal triangle. Dotted lines mark the location of system points characterized by partial wetting at all $T \leqslant T_c$. Dashed lines are projections of tricritical wetting manifolds and solid lines set the boundary for systems showing total wetting in one interface at all temperatures. Labels indicate the nature of the intruding phase and the type of wetting regime in each region (full classification follows by symmetry).

The position of the boundary between type II and type III wetting regimes, corresponding to "tricritical" wetting, was established only for several points, and with a numerical precision of 10^{-2} in the scale of the energy parameters. The characterization of this region is difficult as the discontinuity in the temperature derivative of the equilibrium interfacial tension at the first-order transition is rather small. Our classification also applies to system points in the shield zone, although there are differences in the nature of the wetting phase on each of the three-phase coexistence branches arising from the quadruple point (we will not consider these details here). The distribution of wetting types in the energy space of the model is in full agreement with the qualitative picture of Dietrich, Schick,[8] and Latz[9] for possible wetting behaviors in the BEG model.

It is interesting to note that in spite of the close similarity between the global phase diagrams of binary van der Waals mixtures and this regular mixture-type model, their global wetting diagrams differ both in the location of the boundaries between wetting regimes and the possible order of the wetting transitions. Although the global structure is quite similar,[7] for van der Waals mixtures the boundary between regimes of type I and type II is set by systems whose interaction parameters are related by a geometric mean rule $[\alpha_{12}=(\alpha_{11}\alpha_{22})^{1/2}$, $c=1/2\pm(ab)^{1/2}$ in our language], and second-order transitions are confined to isolated "immiscibility" points (Sullivan limit). Tarazona *et al.*[17] have also found second-order wetting transitions in regions of the interaction space where the van der Waals model predicts first order. Their results correspond to a mean-field model mixture of hard spheres with equal-ranged attractive potentials. The differences between these models have been attributed[7] to the particular way of dealing with the short-ranged repulsions in the van der Waals model (where the range of the repulsions is reduced to a point in the scale in which the attractive potentials vary). The lattice nature of our approach seems to introduce the same kind of perturbations that Costas *et al.*[7] associate to the nonlocal contributions of the molecular repulsions.

Many of the experiments on wetting in binary mixtures have been done on sets of binary mixtures which share one common component while the other is changed within a homologous series. Although we cannot expect the properties of each of these mixtures to be well represented by a unique point (a,b,c) in the energy triangle of our simple model, it is reasonable to assume that a trajectory of points in the energy space will mimick, at least qualitatively, the evolution of gross bulk and surface features characterizing the set. Here we will follow this argument in detail as it will be useful in our analysis of the self-associating case.

Consider the set of binary mixtures: YX, with unnormalized energy parameters (a,b,c); YX_1, with unnormalized energy parameters $(a_1=a,b_1,c_1)$;... and to YX_i, with unnormalized energy parameters $(a_i=a,b_i,c_i)$. Let us take $a+b+c=1$ (assuming $a,b,c>0$) to set our temperature scale. The bulk and surface properties of all the mixtures can be derived by normalizing the corresponding energy parameters and by identifying their location in the energy triangle spanned by (a,b,c). Nevertheless, in order to maintain the same temperature scale and hence to assure a consistent comparison, all relevant features for a single mixture should be displaced by the normalizing factor $[1+(b_i-b)+(c_i-c)]T$ in the temperature scale. The set of points (a_i,b_i,c_i) for the set of mixtures YX_i defines a trajectory in the energy space of our model. We can locate the wetting transition temperature and critical end point for each member of the set, and then it is possible to follow the behavior of these features as a function of the energy parameters. We have made cuts along possible trajectories in the general field space to generate phase diagrams like those depicted in Figs. 4 and 5, where the location of wetting transitions and critical points for three-phase coexistent states are shown in an (*energy parameter*, *temperature*) space. These kind of representations were first introduced by Robledo in his study of the wetting properties of microemulsion lattice models[18] and are analogous to the field phase diagrams of Nakanishi and Fisher[5] and Costas *et al.*[7] As in the latter case, we are limited by construction to the regime of marginal surface enhancements $(g_{ij}=0)$[5]. Our results correspond to the case $h=0$, with h taken as a measure of the departure in the (μ_x,μ_y) space from the line of three-phase coexistence states.

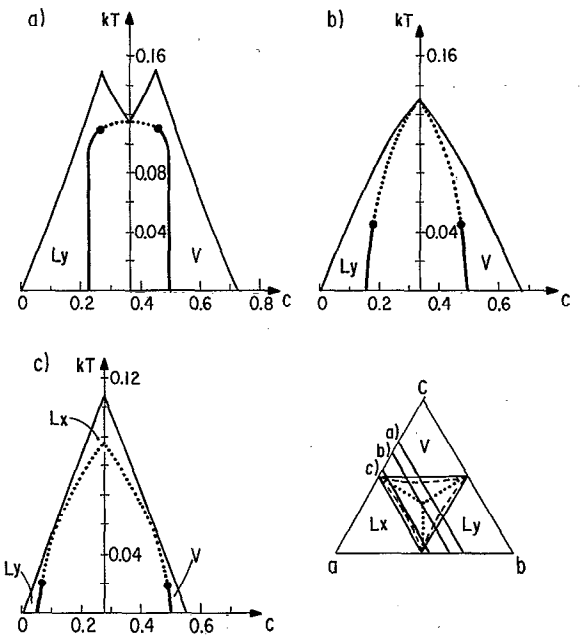

FIG. 4. Field phase diagrams (c,kT) at constant a. (a) $a=0.275$; (b) $a=1/3$; (c) $a=0.45$. Internal solid and dotted lines correspond to first- and second-order wetting transitions, respectively. External solid lines represent critical points for three-phase states. We show the projection of each field space cut onto the principal triangle.

Figure 4 shows cuts along those trajectories projected in the added reference triangle. They correspond to particular cases where $b+c=b_i+c_i$, so the normalized $a_i(=a)$ remains constant in each set (all systems lead to the same temperature scale). External solid lines represent the intersections with critical manifolds for three-phase coexistent states; tricritical points appear like "cusps" in this representation, and they indicate a change in the nature of the phases

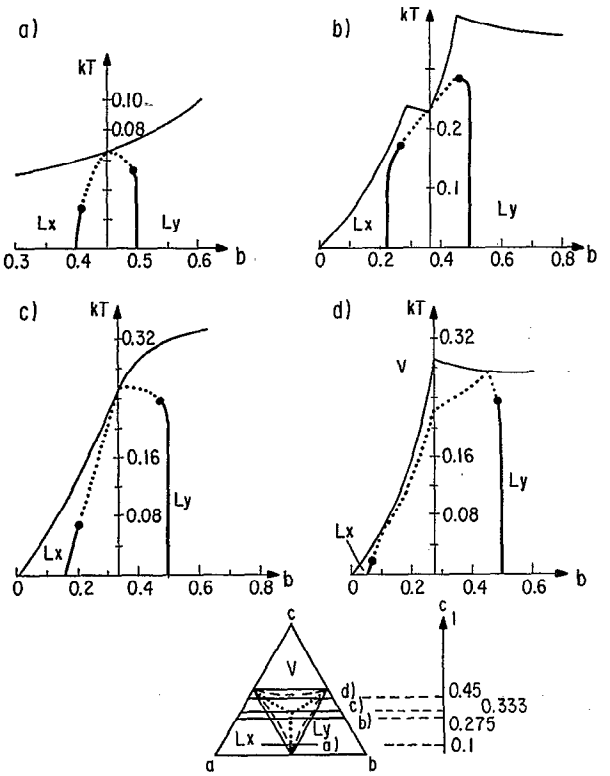

FIG. 5. Field phase diagrams (b,kT) at constant c. (a) $c=0.1$; (b) $c=0.275$; (c) $c=1/3$; (d) $c=0.45$. The notation is described in Fig. 4.

that become critical at critical end points (see Fig. 1). Internal solid lines locate wetting first-order transition temperatures, and dotted lines correspond to second-order wetting transitions. Both type of internal lines merge at tricritical wetting points marked by gross dots. Partial wetting is to be found in the region enclosed by the wetting lines, while total wetting is confined to the region between wetting and critical lines. We indicate in each case the nature of the wetting phase. In Fig. 5 we have chosen trajectories where the normalized $c_i(=c)$ remains constant and the former general description applies. Although there are many other possibilities, these two cases, i.e., a and c constant, summarize the most relevant facts and serve as a basis to generate the structure associated with any other cut (Figs. 1 and 3 are useful in locating the most relevant bulk and surface features, respectively). Both set of diagrams illustrate the sometimes intricate relation between critical and wetting temperatures in this two-order parameter model.

Figures 4 and 5 exhibit some features that are artifacts of the mean-field approximation and the short-ranged interaction model we have employed. The order of the predicted wetting transitions and the symmetry between wetting and "drying" behavior are two of the most remarkable.[4] We expect, however, the underlying connectivity among critical and wetting manifolds to be qualitatively representative of that in real systems. Mean-field short-ranged models for binary systems lead to global phase diagrams[12,19] and possible interfacial behaviors[8,9] that are qualitatively similar to those of more realistic models. This agreement remains as long as

TABLE I. Interfacial data for n-alcohols $(X_i)+C_7F_{14}$ (Y).[a]

n	$\gamma_Y \rightarrow \gamma_a$	$\gamma_{X_i} \rightarrow \gamma_b$	$\gamma_{YX_i} \rightarrow \gamma_c$	T_w	T_c
1	13.1→0.238	22.55→0.410	19.3 →0.351	355.15	430.15
2	13.1→0.245	22.32→0.418	17.98→0.336	335.15	399.15
3	13.1→0.237	23.70→0.428	18.57→0.335	295.85	404.15
4	13.1→0.232	24.57→0.435	18.81→0.333	280.65	404.15
6	13.1→0.225	25.48→0.438	19.52→0.336	256.15	427.15

[a] γ(mN/m) from Refs. 20 and 21, T (K).

the radii of component particles are not too different. In that sense one can surmise that they all will reflect the same basic topology. If every single real mixture in our homologous set were to be represented by a single point (a_i,b_i,c_i) in the energy space, its general behavior could be predicted by following a vertical line in these diagrams. More realistically, this behavior is given by a curve whose path depends on the chemical potentials of both components and the temperature. Despite this, the global behavior of the whole set of mixtures should probe, at least partially, a wide region of the field space and hence it will resemble one of the cuts displayed in Figs. 4 and 5.

To test our assumption, we have analyzed the reported experimental results for sequences of binary mixtures. Guided by the relations in Eq. (7) and by the kind of empirical rules used by experimentalists to set their predictions on wetting behavior, we chose to represent these results on the experimental "energy space" spanned by $(\gamma_X,\gamma_Y,\gamma_{XY},T)$. Here, γ_X and γ_Y are the surface tensions of the pure liquids X and Y, respectively, and γ_{XY} is the interfacial tension between their coexisting liquid phases. The values of these tensions[20] for mixtures of normal alcohols with the fluorocarbon perfluoromethylcyclohexane (C_7F_{14}), e.g., are listed in Table I together with the wetting results of Schmidt.[21] We have normalized the surface and interfacial tensions so that the normalized values $\gamma_a+\gamma_b+\gamma_c=1$; their values are also included in Table I. This set of mixtures seems to define a trajectory in the energy space characterized by the constancy of $\gamma_c(\approx 1/3)$. Figure 6(a) shows the location of the experimental critical and wetting transition temperatures as a function of γ_b. If we let the set $(\gamma_a,\gamma_b,\gamma_c)$ play the role of (a,b,c) in our model [in view of Eq. (7), this is a reasonable assumption when the tension data correspond to temperatures far away from the critical point, and the mixtures are highly insoluble], the predicted behavior is close to that illustrated in Fig. 6(b). Comparison between both figures indicates that the predictions of the model are qualitatively correct, both in the nature of the wetting phase L_y and in the relative trend of critical and wetting transition temperatures (even the deviation for the methanol mixture is expected if we notice that $\gamma_c>1/3$ in this case).

We have applied the same analysis to the experimental results for *water–alkane* mixtures and *methanol–alkane*[22] mixtures finding similar agreement. The last case maps onto a trajectory in the energy space of our model close to that sketched in Fig. 5(a). The model predicts both the inversion in the nature of the wetting phase,[22] and the change in the relative trend of critical and wetting transition temperatures[23]

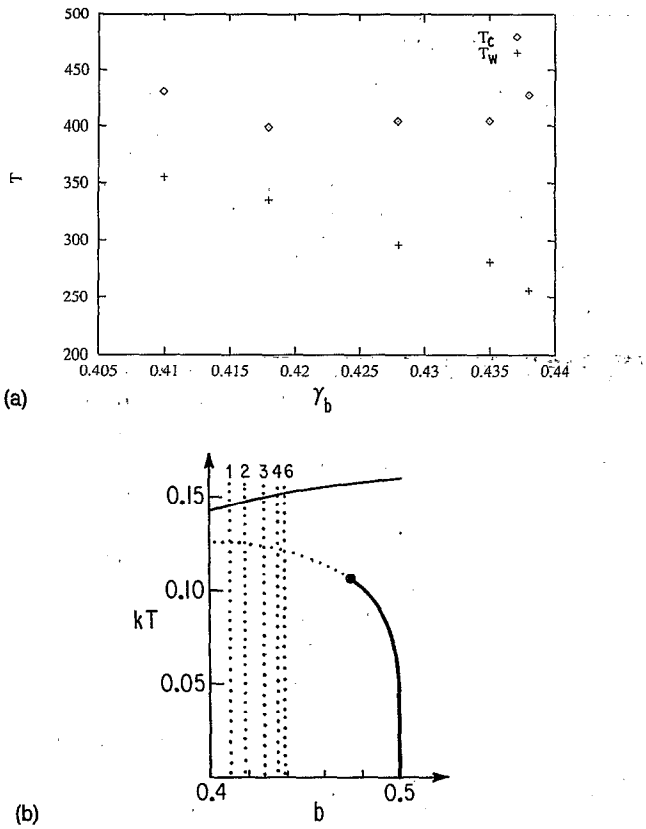

FIG. 6. (a) Critical temperatures T_c and wetting transition temperatures T_w for *n-alcohol*+C_7F_{14} mixtures as a function of the reduced tension γ_b of *n-alcohols*. Total wetting by the fluorocarbon-rich phase (L_y) is found between the two sets of points (data from Refs. 20 and 21). (b) Field phase diagram (b,kT) at constant $c=1/3$ in the range $0.4\leq b\leq 0.5$. The vertical dotted lines indicate the predicted location of each *n-alcohol* (X_i). L_y is the wetting phase in this region.

as b(or γ_b) is increased. The gross wetting behavior of these binary mixtures is conditioned by the relative values of the interfacial tensions, and the present mean-field model seems to capture the basic features. At this level of prediction the perturbations introduced by real experimental conditions like purity of the samples, gravity and finite size effects, relaxation times, etc., do not appear to have a significant influence. Experimental results for this kind of binary mixture or even ternary mixtures are sometimes analyzed in terms of the one-order parameter theory of critical point wetting developed by Cahn.[21,22] This can lead to contradictions that are avoided by working with a two-order parameter theory like the one described here. It accounts for the nonmonotonic or opposite trends observed in most of the cases.

In all the former real mixtures, one of the components is able to show self-association. To what extent this phenomenon modifies the characteristics of wetting is the central problem we address in Sec. III.

III. SELF-ASSOCIATION IN BINARY MIXTURES

A. The model

Consider now a compressible ternary mixture of X, Y, and W components, where species W appears as a result of the process

$$n\mathrm{X}\rightleftharpoons\mathrm{W} \tag{8}$$

with n being a mean aggregation number. Let us associate to this chemical equilibrium the equilibrium constant

$$K_{\mathrm{eq}}=e^{-(\mu_w^0-n\mu_x^0)/kT}=e^{-\Delta G^0/kT} \tag{9}$$

with $\Delta G^0=\mu_w^0-n\mu_x^0$, the standard Gibbs free energy for the (equilibrium in) Eq. (8) referred to a hypothetical ideal solution state. It can also be written in terms of the standard enthalpy (ΔH^0) and entropy (ΔS^0) for the same process ($\Delta G^0=\Delta H^0-T\Delta S^0$).[10,11]

As a generalization of Eq. (1), the mean-field Helmholtz free energy density f_{SA} is given by

$$\begin{aligned} f_{SA}=F_{SA}/N=kT[x\ \ln x+y\ \ln y+w\ \ln w+z\ \ln z] \\ +q[ayz+bxz+cxy+dyw+exw+fwz]+\mu_x^0 \\ +\mu_y^0+\mu_w^0, \end{aligned} \tag{10}$$

where $N=N_x+N_y+N_w+N_z$, w and μ_w^0 represent the occupation density and standard chemical potential of the new species, and

$$d=\alpha_{yy}+\alpha_{ww}-2\alpha_{yw},\quad e=\alpha_{xx}+\alpha_{ww}-2\alpha_{xw},\quad f=\alpha_{ww}$$

are a measure of the additional interactions in the system.

The chemical potentials are derived from Eq. (10) as

$$\left(\frac{\partial f_{SA}}{\partial x}\right)_{y,w}=kT\ \ln(x/z)+qb(z-x)+q(c-a)y+q(e-f)w+\mu_x^0=\mu_x, \tag{11a}$$

$$\left(\frac{\partial f_{SA}}{\partial y}\right)_{x,w}=kT\ \ln(y/z)+qa(z-y)+q(c-b)x+q(d-f)w+\mu_y^0=\mu_y, \tag{11b}$$

$$\left(\frac{\partial f_{SA}}{\partial w}\right)_{x,y}=kT\ \ln(w/z)+qf(z-w)+q(e-b)x+q(d-a)y+\mu_w^0=\mu_w. \tag{11c}$$

The global phase diagram for the self-associating mixture can be outlined by analyzing the intersections of the phase coexistence and critical manifolds defined by Eqs. (10) and (11), with the additional chemical restriction imposed by the law of mass action:

$$n\mu_x-\mu_w=0.$$

Using Eqs. (11),

$$\begin{aligned} kT\ \ln\left[\frac{wz^{n-1}}{x^n}\right]+qa(n-1)y+qb[(n-1)x-nz] \\ +q[d-nc]y+qe[x-nw]+qf[z+(n-1)w] \\ +\Delta G^0=0 \end{aligned} \tag{12}$$

with $z=1-x-y-w$.

Surface properties are obtained following the same procedures described above. The grand potential per number of sites in a plane for the inhomogeneous system is

$$\omega=\sum_{i}^{N_p}(f_{SA}^{i}-a\Delta y\Delta z-b\Delta x\Delta z-c\Delta x\Delta y-d\Delta y\Delta w$$

$$-e\Delta x\Delta w-f\Delta w\Delta z-\mu_x x-\mu_y y-\mu_w w) \quad (13)$$

with i running over N_p planes. The minimization conditions are

$$\mu_x=\mu_x^i-b(\Delta^2 z-\Delta^2 x)-(c-a)\Delta^2 y-(e-f)\Delta^2 w, \quad (14a)$$

$$\mu_y=\mu_y^i-a(\Delta^2 z-\Delta^2 y)-(c-b)\Delta^2 x-(d-f)\Delta^2 w, \quad (14b)$$

$$\mu_w=\mu_w^i-b(\Delta^2 z-\Delta^2 w)-(e-b)\Delta^2 x-(d-a)\Delta^2 y, \quad (14c)$$

where f_{SA}^i, μ_x^i, μ_y^i, and μ_w^i represent the Helmholtz free energy density and chemical potentials, respectively, of a uniform system with densities $x_i,y_i,w_i(z_i=1-x_i-y_i-w_i)$. Surface tensions for pairs of coexisting phases are calculated from the solution profiles for Eqs. (14) under the adequate boundary conditions.

B. Results

The global phase diagram for this compressible three-component model is not known and one can expect it to be complex in its details. We have simplified the task of calculating phase diagrams by considering cases where $e=0$, i.e., by assuming that no segregation is induced by the interaction between species X and its aggregate W, while all other energy parameters are taken to be always greater than zero. Three-phase coexistence surfaces in the field space (μ_x,μ_y,μ_w,T) are then generated as extensions of triple point lines for what we will call the binary mixture limits, YX ($\mu_w\to-\infty$) and YW ($\mu_x\to-\infty$). Phase coexistence states for the self-associating case are found by analyzing the intersections of these manifolds and the chemical equilibrium surface defined by Eq. (12). As for the binary mixture, once a coexistence point satisfying physical and chemical equilibrium conditions is found, the structure of equilibrium profiles for pair of coexisting phases are unequivocally determined and so are the corresponding wetting properties. Although we studied several combinations of the physical energy parameters (a,b,c,d,f) and chemical parameters $(\Delta H^0,\Delta S^0)$, here we summarize the results for a set of cases which is fairly representative of the general behavior. It is important to mention that in this study of self-associating mixtures we have considered cases where the process of association has little influence in the structure of the bulk phase diagrams. In any other situation, the presence of new phases or critical points can modify our conclusions.

Given a system with parameters (a_i,b_i,c_i,d_i,f_i), the behavior of the binary limits YX and YW can be obtained by locating in the barycentric representation of the binary mixture energy space the renormalized points $(a_i/\Sigma_{xy}=a,\ b_i/\Sigma_{xy}=b,\ c_i/\Sigma_{xy}=c)$ with $\Sigma_{xy}=a_i+b_i+c_i$ and $(a_i/\Sigma_{yw}=a',\ f_i/\Sigma_{yw}=f,\ d_i/\Sigma_{yw}=d)$ with $\Sigma_{yw}=a_i+f_i+d_i$. Any of these normalized sets can then be used to define a temperature scale. To further simplify our scanning of possible behaviors, we have selected symmetrical mixtures where $c=d$ (the solvent Y does not distinguish X from W) and we have chosen to work with systems where the self-associating process is favored at low temperatures ($\Delta H^0<0$) but not at high temperatures ($\Delta S^0<0$). So, for $T=0$, all mixtures are in the binary limit YW with coexisting phases L_y,L_w,V at the triple point. As the temperature is increased, W is replaced gradually by species X at a rate that depends on the particular value of the physical and chemical parameters. Numerical calculations were carried out with an aggregation number $n=4$ taken as a representative value for self-associating systems like linear alcohols.[24] For each chosen set of physical parameters, triple point lines have been followed for several values of ΔH^0 and ΔS^0. Critical points and wetting transition temperatures are located through the same kind of procedures described in Sec. II B. By changing ΔH^0 and ΔS^0 we are able to scan the basic connectivity of critical and wetting transitions of the underlying three-component system.

Given the structure and behavior of Eqs. (1) and (10) for the Helmholtz free energy of simple and self-associating binary mixtures, we find it convenient to represent our results as a function of an "effective" interaction defined by

$$b_{\text{eff}}=\frac{bx_s+fw_s}{x_s+w_s}, \quad (15)$$

where x_s and w_s are densities in the $L_{w\to x}$ coexisting phase rich in species W or X; b and f should be seen as limit values for the mean interaction energy between self-associating species. Figures 7 and 8 show the evolution of critical and wetting transitions temperatures as a function of b_{eff} for particular mixtures. The trajectories indicated by arrows correspond to different sets of values of $(\Delta H^0,\ \Delta S^0)$ and each one represents the temperature behavior of a single system. All other points were located following similar trajectories always bounded by the low $(f\to\alpha_{ww})$ and the high $(b\to\alpha_{xx})$ temperature limits of b_{eff}. It can be seen from these figures that the presence of self-association induces unexpected wetting behavior. Consistent with the idea that self-association is favored in solution, we have taken $f>b$ in these examples.

Following the lower path in Fig. 7, we find that the system can go through the sequence *total→partial→total* wetting by the L_y phase. This is an example of reentrant wetting. For this particular model the order of the wetting transitions is first order at lower temperatures and second order at higher temperatures. By favoring the self-association process (increasing ΔS^0, for example), we recover the wetting properties of the binary mixture limit YX determined by the value of f for given d. In Fig. 8 the reentrant wetting behavior involves an inversion in the nature of the wetting phase, and it can be conceived as dewetting: we go from total wetting by the phase L_y at low temperatures to total drying by the same phase as the temperature increases (or total wetting by the L_x phase). The order of the transitions depends on the value of ΔH^0 and ΔS^0. In these examples b and f have been chosen to assure visiting different wetting sections. In real mixtures, however, even if the strength of molecular interac-

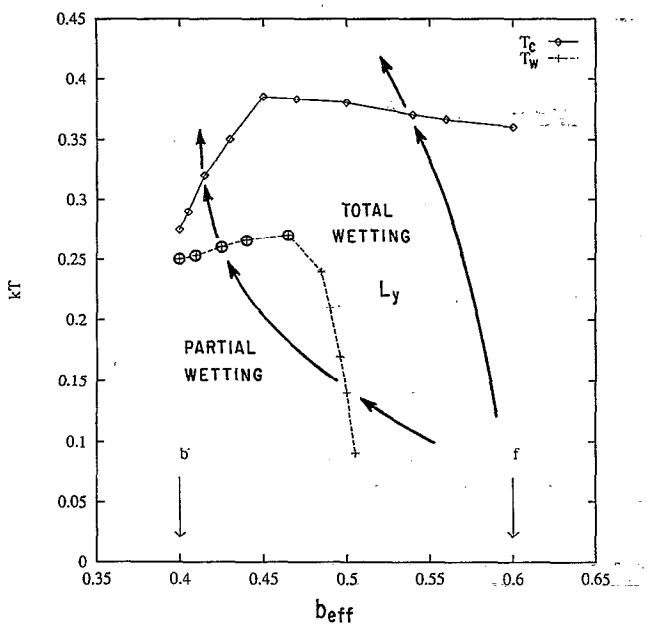

FIG. 7. Field phase diagram for self-associating mixtures with $a=0.325$, $b=0.4$, $c=0.275$ and $a'=0.125$, $f=0.6$, $d=0.275$. The solid line traces the location of critical temperatures T_c; dashed lines trace the location of wetting temperatures. Wetting transitions are marked with crosses that are encircled when the transition is second order. Both trajectories correspond to systems with $\Delta H^0=-1$; $\Delta S^0/k=-7$ in the lower path, $\Delta S^0/k=-4$ in the upper path.

tions characterizing free and aggregate species is not too different, this kind of behavior could be expected if the system energy parameters are located close to boundaries between different wetting regimes.

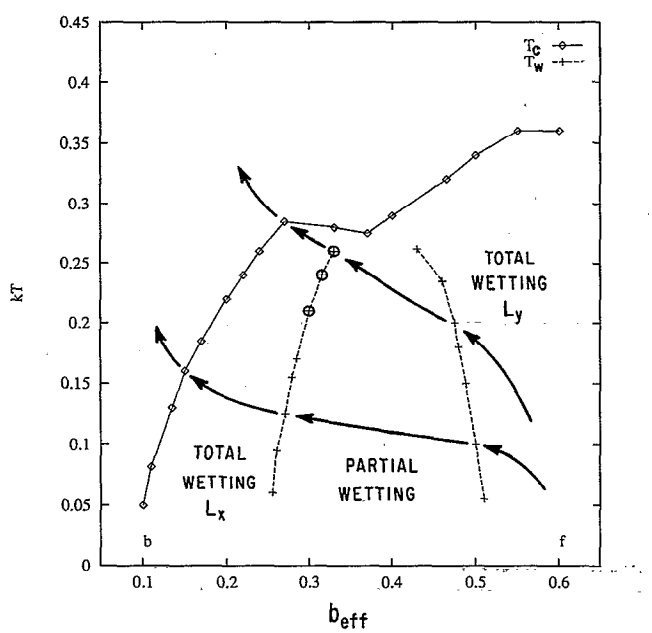

FIG. 8. Field phase diagram for self-associating mixtures with $a=0.625$, $b=0.1$, $c=0.275$ and $a'=0.125$, $f=0.6$, $d=0.275$. ($\Delta H^0=-1$, $\Delta S^0/k=-9$) in the lower trajectory, ($\Delta H^0=-1$, $\Delta S^0/k=-7$) in the upper one. The notation is the same described in Fig. 7.

We would like to emphasize the close qualitative similarity between the field phase diagrams in Figs. 7 and 8 and the appropriate sections of Fig. 5(b) corresponding to a cut at constant c in the binary mixture field space. This is a general result for all system phase diagrams we have analyzed. In all cases we were able to predict the qualitative behavior of the self-associating system by drawing temperature-dependent trajectories, like those in Figs. 7 and 8 between the chosen limits of b and f, on field space cuts of the binary problem for the selected value of $c=d$. Our results indicate that similar conclusions apply for different parameter restrictions, with "reentrant wetting" and "dewetting" as the most relevant unexpected features. Under many conditions individual self-associating binary mixtures behave like a continuous set of simple binary mixtures in a homologous YX_i series, where the nature of X_i changes with temperature. The analogy is better the closer the set of physical parameters defining the binary mixture limits are in the energy space.

In the context of our model, self-association increases the probability of dealing with first-order wetting transitions as the system gains freedom to move across the field space. First-order transitions are always better defined (the discontinuity in the derivative of the equilibrium tension is higher) than in the simple binary mixture case.

If self-association is going to have any identifiable influence on the wetting behavior of a mixture, it will be on systems where the association process is strongly temperature dependent and has a considerable impact on the strength of relevant molecular interactions. Moreover, the relative balance of these interactions should assure that the system will be driven across different wetting regimes. The possible effect of self-association on the experimental systems described in Sec. II B is then not clear. Experimental results for self-association in linear alcohols,[23] e.g., show that we can expect all mixtures of a given compound with members of this homologous series to have their wetting properties affected in the same degree. This would imply just a general shift of the results with respect to those predictions based on a simple binary mixture model. Within our qualitative approach, the effect cannot be noticed.

IV. SUMMARY AND CONCLUSIONS

In Sec. II B we described the global wetting phase diagram for a simple binary mixture represented by a mean-field spin-1 Ising model. We have pointed out that in spite of the susceptibility of wetting properties to the details of molecular interactions, we expect the general evolution of critical and wetting transition manifolds to be close to that for more realistic approaches. In that sense, the kind of field space cuts depicted in Figs. 4 and 5 are useful in analyzing the gross behavior of real systems. Some of the trends summarized in these pictures have been observed when working with different sets of binary mixtures, and recent experimental results[23] show the advantages of taking this model as a guiding approach. Although experimental studies of interfacial wetting have explored a small subset of possible binary mixtures, it seems that there is just a limited number of general wetting behaviors and that their coarse features are captured by the simple model we present here.

The knowledge of the wetting properties of the simple binary mixture model simplified the task of characterizing the wetting behavior of our crude model for self-associating systems. For this case, we have just presented a general overview consistent with our interest in understanding the possible unexpected behaviors that can occur as a result of self-association in the medium. We have found that under adequate circumstances, the presence of an association equilibrium can be responsible for irregular wetting behavior, such as reentrant wetting or dewetting. The extent to which this process is responsible for some of the unexpected experimental results in binary mixtures with one self-associating component[25] should be the subject of further theoretical and experimental work. Under the conditions described in this work, the appearance of a third species in solution does not seem to add any relevant topological feature, but enriches the set of possible behaviors by allowing a system point to follow different trajectories along an extended field space. In that sense, the interfacial behavior of simple ternary mixtures where two of the species have similar properties should not be far from that which we could predict following appropriate trajectories at constant temperature on field space cuts of the binary problem.

ACKNOWLEDGMENTS

We would like to thank Miguel Costas for his very helpful ideas and for fruitful discussions, and Ma. Eugenia Costas and Carey Bagdassarian for their comments on the manuscript. We thank also the Consejo Nacional de Ciencia y Tecnología de México (Grant No. 0679-E9111) for their financial support. V. Talanquer appreciates the support from the James Franck Institute at the University of Chicago.

[1] J. W. Cahn, J. Chem. Phys. **66**, 3667 (1977).
[2] C. Ebner and W. F. Saam, Phys. Rev. Lett. **38**, 1486 (1977).
[3] D. E. Sullivan and M. M. Telo da Gama, in *Fluid Interfacial Phenomena*, edited by C. A. Croxton (Wiley, New York, 1986).
[4] S. Dietrich, in *Phase Transitions and Critical Phenomena*, edited by C. Domb and J. L. Lebowitz (Academic, New York, 1988), Vol. 12.
[5] H. Nakanishi and M. E. Fisher, Phys. Rev. Lett. **49**, 1565 (1982).
[6] R. Pandit and W. Wortis, Phys. Rev. B **25**, 3226 (1982).
[7] M. E. Costas, C. Varea, and A. Robledo, Phys. Rev. Lett. **51**, 2394 (1983).
[8] S. Dietrich and M. Schick, Phys. Rev. B **33**, 4952 (1986).
[9] S. Dietrich and A. Latz, Phys. Rev. B **40**, 9204 (1989).
[10] L. R. Corrales and J. C. Wheeler, J. Chem. Phys. **91**, 7097 (1989).
[11] V. Talanquer, J. Chem. Phys. **96**, 5408 (1992).
[12] D. Furman, S. Dattagupta, and R. B. Griffiths, Phys. Rev. B **15**, 441 (1977).
[13] N. Blume, V. Emery, and R. B. Griffiths, Phys. Rev. A **4**, 1071 (1971).
[14] V. Talanquer, C. Varea, and A. Robledo, Phys. Rev. B **39**, 7016 (1989).
[15] J. W. Cahn and J. E. Hilliard, J. Chem. Phys. **28**, 258 (1958).
[16] J. S. Rowlinson and B. Widom, *Molecular Theory of Capillarity* (Clarendon, Oxford, 1982).
[17] P. Tarazona, M. Telo da Gama, and R. Evans, Mol. Phys. **49**, 283 (1983).
[18] A. Robledo, *Statistical Models for Micellar Solutions and Microemulsions*, Supplement to the Proceedings of the Fourth Mexican School on Statistical Physics, 1987 (World Scientific, Singapore, 1989).
[19] R. L. Scott and P. H. van Konynenburg, Discuss. Faraday Soc. **49**, 81 (1970); P. H. van Konynenburg and P. L. Scott, Philos. Trans. R. Soc. London Ser. A **298**, 495 (1980).
[20] *CRC Handbook of Chemistry and Physics*, 62nd ed. (Chemical Rubber, Boca Raton, FL, 1981).
[21] J. W. Schmidt, J. Colloid Interface Sci. **122**, 575 (1987).
[22] M. Kahlweit, G. Busse, D. Haase, and J. Jen, Phys. Rev. A **38**, 1395 (1989).
[23] E. Carrillo-Nava and M. Costas (private communication, unpublished results).
[24] L. Andreoli-Ball, D. Patterson, M. Costas, and M. Cáceres-Alonso, J. Chem. Soc. Faraday Trans. 1 **84**, 3991 (1988).
[25] P. G. de Gennes, Rev. Mod. Phys. **57**, 827 (1985).